Chapter 2

FORMATION OF LIQUID CRYSTALLINE PHASES FROM A LANGMUIR MONOLAYER

2.1 Introduction

This chapter deals with studies on a monolayer of 4' -n -octyl-4-cyanobiphenyl (8CB) at the air-water interface. The molecular structure of the compound is shown in Fig 2.1. In bulk, 8CB is a liquid crystal forming compound and shows the following phase sequence.

$$Crystal \xrightarrow{20.5°C} SmecticA \xrightarrow{33.3°C} Nematic \xrightarrow{41.5°C} Isotropic.$$

Many liquid crystal forming molecules are known to form stable Langmuir monolayers [1, 2, 3]. Molecules that form liquid crystals in bulk are generally rodlike in structure. Hence their interparticle interactions are simpler than those between conventional long chain surfactant molecules [4]. This brings in the likelihood of new phases, making these molecules an interesting system. In addition, the presence of smectic phase in some of these materials brings in an interesting possibility of layer orderings at the air-water interface. There has been a lot of work on such monolayers going over into organised multilayer films on compression [4, 5, 6, 7], instead of going into denser phases as seen for other molecules [3]. Xue *et.al.* [4] studied the 8CB monolayer using surface manometry, ellipsometry

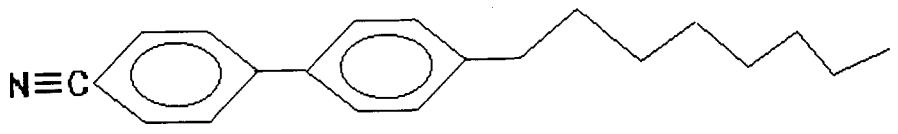

Figure 2.1 Molecular structure of Octyl-cyanobiphenyl (8CB).

and optical second harmonic generation. They report a first order phase transition from the homogeneous monolayer to a stable three layer phase at the air water interface. Friedenberg *et.al.* *[5]* and Mul and Mann [6] studied the same system using Brewster angle microscopy. They report a similar first order phase transition on compressing the monolayer. Friedenberg *et.al.* also report a smooth transformation of the three layer structure into a monolayer on expansion. Mul and Mann report the formation of thicker domains on further compression of the three layer structure. They also propose a model for the transition from monolayer to three layer structure. Schmitz and Gruler [7] have studied the system using surface potential (AV) measurement. They report an additional second order phase transition after the formation of the three layer structure.

Surprisingly, none of these workers made an attempt to characterise the phases of these 3D domains and correlate the phases seen in bulk 8CB to those seen in the domains at the interface.

Here we give an account of our studies on 8CB films. We employed fluorescence, reflection and polarising microscopy in addition to surface manometry for our studies. We have characterised the phases and surface topography of the thick domains formed at the interface on compressing the Langmuir monolayer.

2.2 Experimental Techniques

2.2.1 Preparation of the Monolayer

The 8CB monolayer was formed on Millipore Milli Q water (resistivity > 18 MΩ) contained in a **35** cm by 10 cm Teflon trough of depth **5** mm. The trough was equipped with a movable barrier used to compress the monolayer to a desired area. The barrier was moved using a computer controlled DC motor, and the movement was tracked using an encoder. A nichrome heater was fitted under the trough to heat the system. The temperature was measured using a Keithley 4 – probe resistance temperature detector. For each experiment the subphase was maintained at a constant temperature to an accuracy of ± **1°C.**

The trough was cleaned thoroughly by leaving it overnight filled with chromic acid. The chromic acid was removed and the trough was rinsed repeatedly with millipore water to remove all traces of the acid. It was considered to be properly clean only when the water completely dewetted the surface on emptying.

The compound 8CB was obtained from BDH, UK and used as received. The monolayer was formed by adding small quantities of dilute (milli molar) 8CB solution in chloroform or hexane onto the water surface using a Hamilton microsyringe. The solvents used were of HPLC or spectroscopic grade, procured from Merck or Ranbaxy and were used as received. Usually, the solvent evaporates almost immediately allowing the solute molecules to form a monolayer. The monolayer was allowed at least **15** to 20 minutes to stabilise. The whole assembly was enclosed in a Perspex box to avoid contamination and air currents.

2.2.2 Surface Manometry

Surface manometry of a monolayer is the measurement of the surface pressure (π) as a function of area per molecule *(A,)* and provides the two dimensional (2D) equivalent of pressure – volume characteristics for bulk systems. This technique was first developed by Pockels [8]who estimated π by measuring the force required

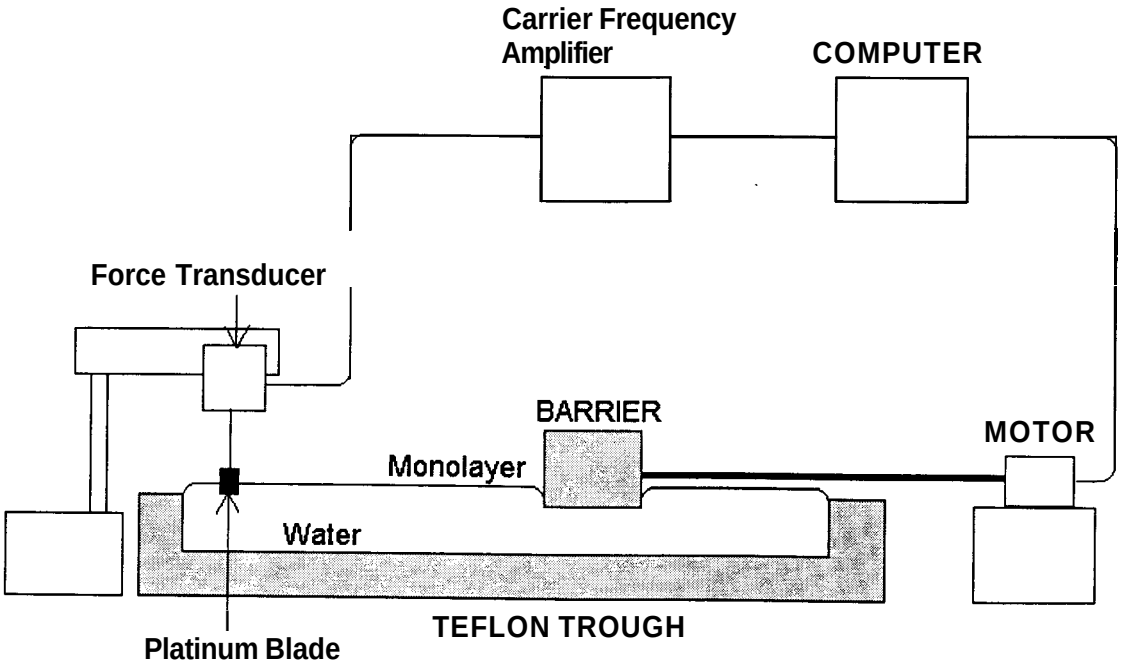

Figure 2.2 Experimental setup used for measuring Surface Pressure by Wilhelmy plate technique.

to pull a button out of the monolayer covered water. Langmuir worked extensively on surface manometry using a film balance [9]. Here a floating barrier of waxed paper was placed across the trough with a clean surface at one end and the monolayer covered surface at the other. The force acting on the barrier was measured using a balance.

With the advent of modern force transducers, the Wilhelmy plate technique [10] has practically taken over from the film balance technique. This is a refinement of the Pockels technique, where one dips a plate (either a platinum blade or a filter paper) into the water. The plate is suspended by a thin wire from a force transducer which measures the force acting on it, as shown in Fig 2.2. The total force acting on the plate (Fig **2.3)** is given by

$$F = 2l\gamma + mg - F_B \tag{2.1}$$

where F_B = the force of buoyancy on the plate;

1 = length of the plate;

γ = surface tension of the water; and

m = mass of the plate.

The factor 2 comes to account for the two edges of the platinum plate. At the

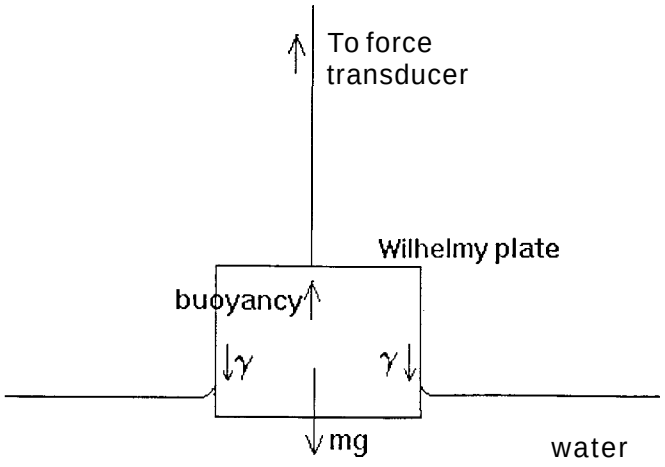

Figure **2.3** Schematic representation of the forces acting on the Wilhelmly plate.

beginning of the experiments, the plate is dipped in pure water to obtain

$$F_o = 2l\gamma_o + mg - F_B \tag{2.2}$$

where γ_o = surface tension of pure water. After the monolayer is spread, we obtain

$$F = 2l\gamma + mg - F_B \tag{2.3}$$

where γ = surface tension of water with the monolayer. Hence the surface pressure π is given by

$$\pi = \gamma_o - \gamma = (F_o - F)/(2l) \tag{2.4}$$

The force is measured using a transducer which generates an electrical signal proportional to the force. This signal is digitized and recorded in a computer.

We employed the Wilhelmy plate technique for our surface manometry experiments. We measured π by determining the force acting on a platinum blade dipped in water using a force transducer. The experiments were also repeated by replacing the platinum blade with a filter paper, the results obtained were identical. Two force transducers, one from HBM, Germany and a tensiometer from

NIMA, England were used. The surface pressure data was collected on a PC which also controlled the barrier movement. The isotherms were plotted using this value of π against A, calculated from the barrier position. We were able to measure π with an accuracy of $\pm$ 0.1 dyne/cm.

2.2.3 Epifluorescence Microscopy

Epifluorescence microscopy [11] was employed to visually observe the phases in the monolayer. The setup used is shown in Fig 2.4. We used a Leitz Mettalux 3 microscope for our studies. Light from a mercury arc lamp (HBO 100W/2, Osram, Germany) passed through the first filter of the filter system and was reflected downward using the half silvered mirror to strike the monolayer. The filter system is shown in Fig 2.5 (b). The first filter allowed light of wavelengths in the range 4200 to 4900 Å to pass through. The objective of the microscope (Leitz, Metallux 3) focussed the light on the monolayer. The monolayer was doped with a 1% molar concentration of a fluorescent dye 4 - (hexadecyl amino) - 7 - nitrobenz - 2 oxa - 1, 3 - diazole (NBD-HDA, obtained from Molecular probes, USA). This dye is excited by a radiation at $\lambda = 4680$ Å and it fluoresces at $\lambda =$ 5330 Å. The fluorescent light was collected by the microscope objective and went through the second filter. This filter allowed wavelengths above 5100 Å to pass and blocked the light that excited the dye. The resulting fluorescent intensity was very weak and could either be observed visually or recorded on a video recorder using an intensified CCD camera (Model P 46036A/V22, EEV, England).

Here we recall the general features of a dye doped monolayer under the fluorescence microscope. In the gas – LE two phase co-existence region, the gas phase appears dark compared to the LE phase. This is attributed to (i) the low density of the gas phase and hence the low density of dye molecules and (ii) the quenching of the dye in the gas phase [11] due to contact of the chromophore group of the dye with water. In case of 3D domains, the brightness of a domain gives a measure of its thickness.

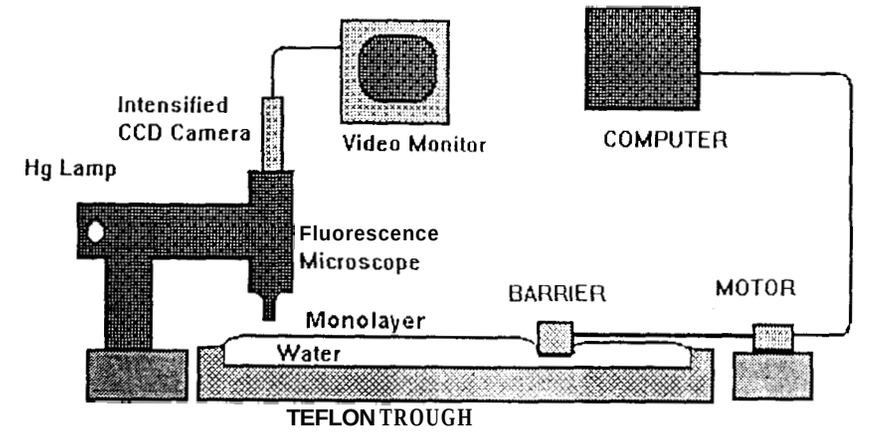

(a)

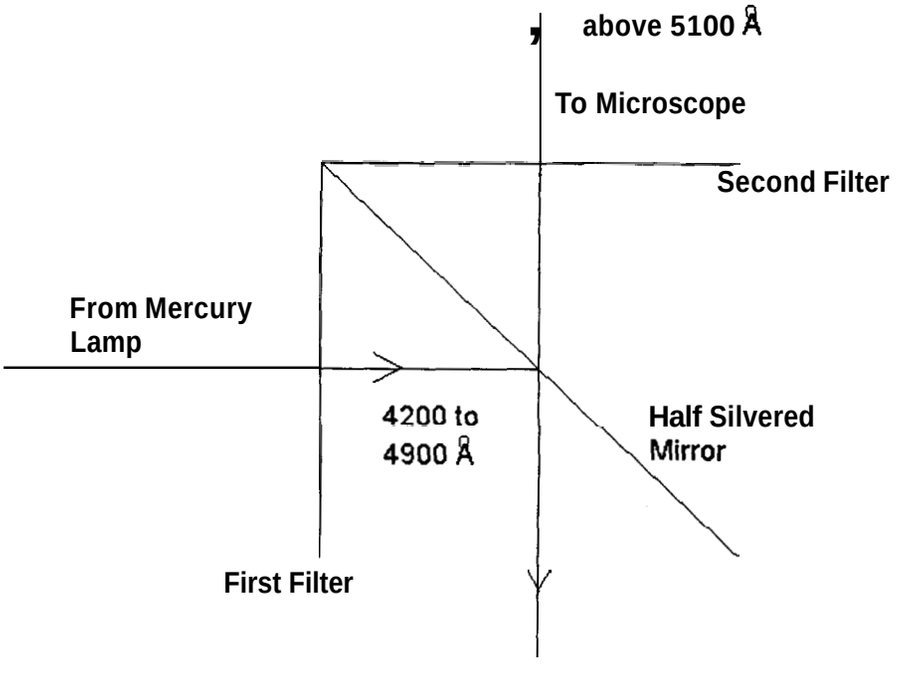

(b)

Figure 2.4 (a) Schematic diagram of the experimental setup for Epifluorescence microscopic studies. (b) Details of the Filter System.

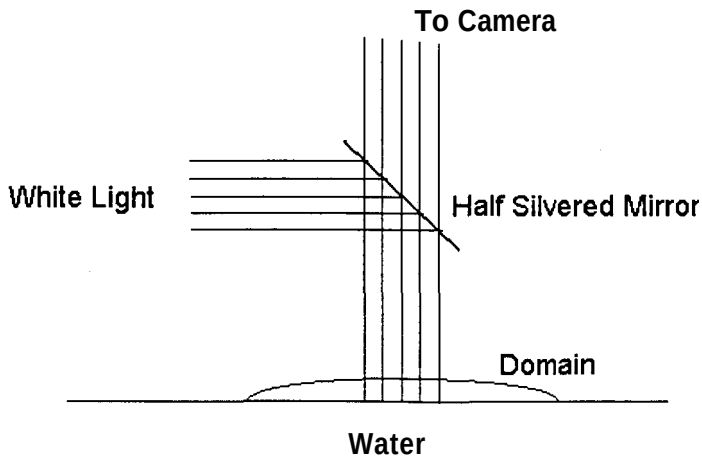

Figure 2.5 A schematic diagram of the reflection microscopy arrangement.

2.2.4 Reflection and Polarising Microscopy

These techniques were used to study the comparatively thicker ($\sim$ 1000 Å) domains formed on compressing the monolayer to very low ***A,.*** Reflection microscopy was used to study the surface topography of the domains. It was done on the Leitz microscope, replacing the filter system with a reflection mode adapter (Fig 2.5). Here white light from the mercury lamp was made to fall on the monolayer and the reflected light was observed.

To be visible under reflection, a domain must have a minimum thickness

$$d = \frac{\lambda}{2\mu'} \tag{2.5}$$

where λ = wavelength of light and μ' = effective refractive index of the domain. Taking $\mu' \sim 1.5$ and $\lambda \sim 5000$ Å, we get d $\sim$ 0.2 μm, which is the necessary minimum thickness to be visible under reflection. Hence, the thin domains were not visible under reflection.

There is a path difference $(2\mu' d)$ between light reflected from the 8CB - air and water - 8CB interfaces. This causes optical interference. The interference is constructive or destructive depending on the wavelength of light. There would be constructive interference for light of certain wavelength that satisfies Equation 2.5. Hence, a flat domain would show a uniform colour all over. On the other

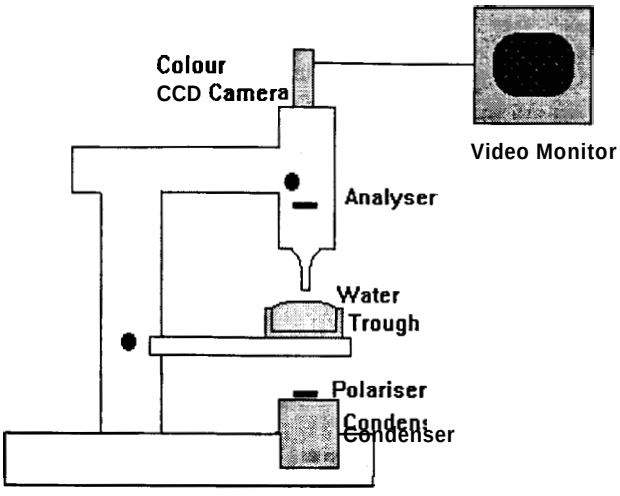

(a)

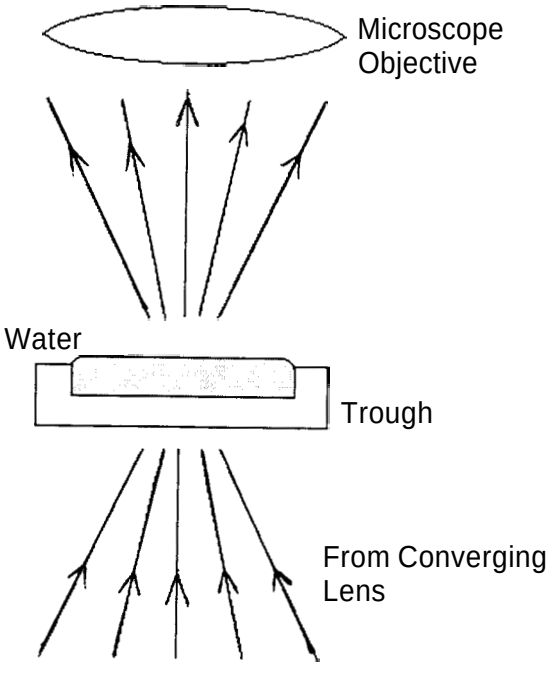

(b)

Figure 2.6 (a) Experimental setup for polarising microscopic studies, (b) The conoscopy setup.

hand, if the thickness of the domain be varying, one would see regions of different colour. For a lens shaped domain, one would see concentric rings, analogous to Newton's rings.

Polarising microscopy was used to observe the textures of the multilayer domains. Here the monolayer was illuminated by a plane polarised parallel beam of white light from below. The emergent light was observed through a crossed analyser as shown in Fig 2.6 (a). The experiments were carried out on a Leitz Orthoplan polarising microscope. The monolayer was formed on water taken either in a circular glass trough (10 cm diameter) or a Teflon trough with a glass window. The reflection and polarising microscopy images were collected using a Sony colour CCD camera.

The domains that appeared textureless under polarising microscope were probed further using the technique of conoscopy (Fig 2.6 (b)). Here the monolayer was illuminated from below by a convergent beam of plane polarised light. The transmitted light was observed through a crossed analyser. An isotropic domain would get extinguished. A domain which is birefringent with the optic axis normal to the air – water interface would exhibit colours as the light would not be passing along the optic axis.

2.3 Results

The $\pi - \mathbf{A}$, isotherms are shown in Fig 2.7. We may recall that in the usual monolayers, the isotherm exhibits a flat region at high **A**, corresponding to the gas – LE two phase co-existence. This is followed by a region of steeply increasing π corresponding to the pure LE phase. After that there is a change of slope, where the LC phase appears. In the isotherms of 8CB, the plateau seen at **A**, greater than 60 Å^2 corresponds to the gas – LE two phase region. The region with steeply increasing π, (**A**, $\sim$ **48** - *55* Å^2) represents the pure LE phase. The region for **A**, less than 48Å^2 corresponds to the formation of multilayers and other 3D domains.

Before starting the compression, the monolayer was allowed to stabilise for at

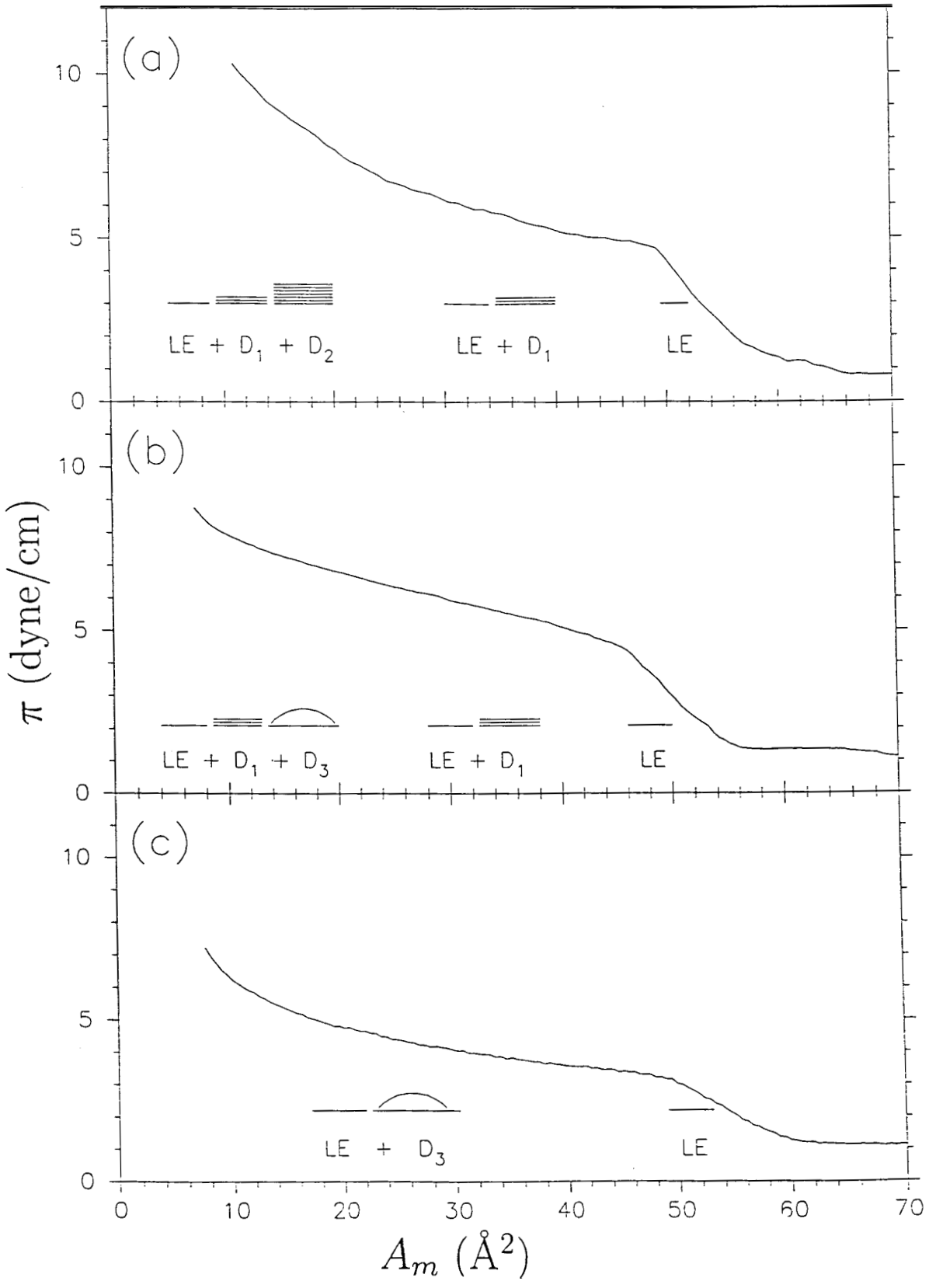

Figure 2.7 Surface Pressure – Area isotherms of 8CB monolayer at different temperatures. (a) 25°C, (b) 35°C and (c) 40°C. The 3D domains formed are shown schematically.

least 15 to 20 minutes. The experiments were also repeated with longer periods of time, in the range of 45 minutes to 1 hour. The isotherms were found to remain identical.

To study the phases indicated by the surface manometry studies, we employed epifluorescence microscopy. Since this involved doping 8CB with the fluorescent dye, we checked that the isotherms of pure and doped monolayers were almost identical. This indicated that the phases seen under fluorescence were not some artifacts of the dye.

We first observed the gas – LE co-existence region under the microscope (Fig 2.8). Here the gas phase appeared dark and the LE phase appeared bright. On compressing the monolayer, the area covered by the LE phase increased at the expense of that covered by the gas phase. The gas phase ultimately disappeared on compressing to 55 $Å^2$ A„ and the whole field of view became uniformly bright.

At 25°C, on compressing the monolayer further, we observed the formation of still brighter domains (D_1) in the LE phase at 48 $Å^2$. In view of earlier studies [4, 5, 6, 7], we expect these domains to be a three layer structure. As can be seen in Fig 2.7(a), π continued to rise in this region, albeit slowly. In this region, the features of the isotherm depended on the compression rate. For fast compressions, (0.1 $Å^2$ /molecule/second) this part of the isotherm was almost horizontal, as reported by Xue *et.al.* [4]. On compressing further, before the D_1 domains could occupy the entire area, still brighter domains (D_2) appeared at 20$Å^2$ (Fig 2.9). The D_2 domains exhibited different intensity levels and mostly appeared near the centre of the D_1 domains (Fig 2.10). Brewster angle microscopy studies [6] under similar conditions indicate the formation of domains of different thicknesses. Accordingly, we suggest that the different intensities of the D_2 domains are due to their different thicknesses. This difference in fluorescence intensity seems to be due to the presence of more molecules of NBD-HDA per unit area in the thicker domains. Interestingly, here we saw the co-existence of LE phase with D_1 and D_2 domains.

In the field of view of the microscope, we could detect defocusing due to a

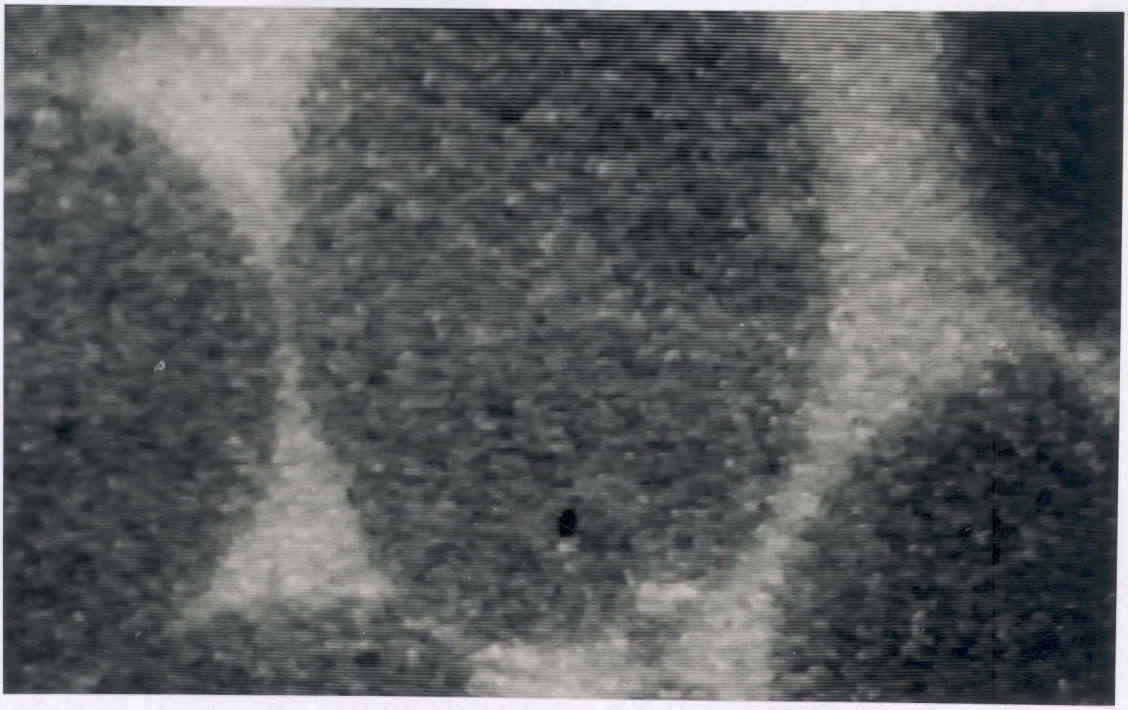

Figure 2.8 Fluorescence image of gas – LE co-existence for a 8CB monolayer at 25°C 70Å^2 A_m. Scale of the image: 1080μm x 750μm.

Figure 2.9 Fluorescence image of 8CB monolayer at 25°C 18Å^2 A_m showing co-existence of LE (black), D_1 (grey) and D_2 (bright) domains. Scale of the image: 1080μm x 750μm.

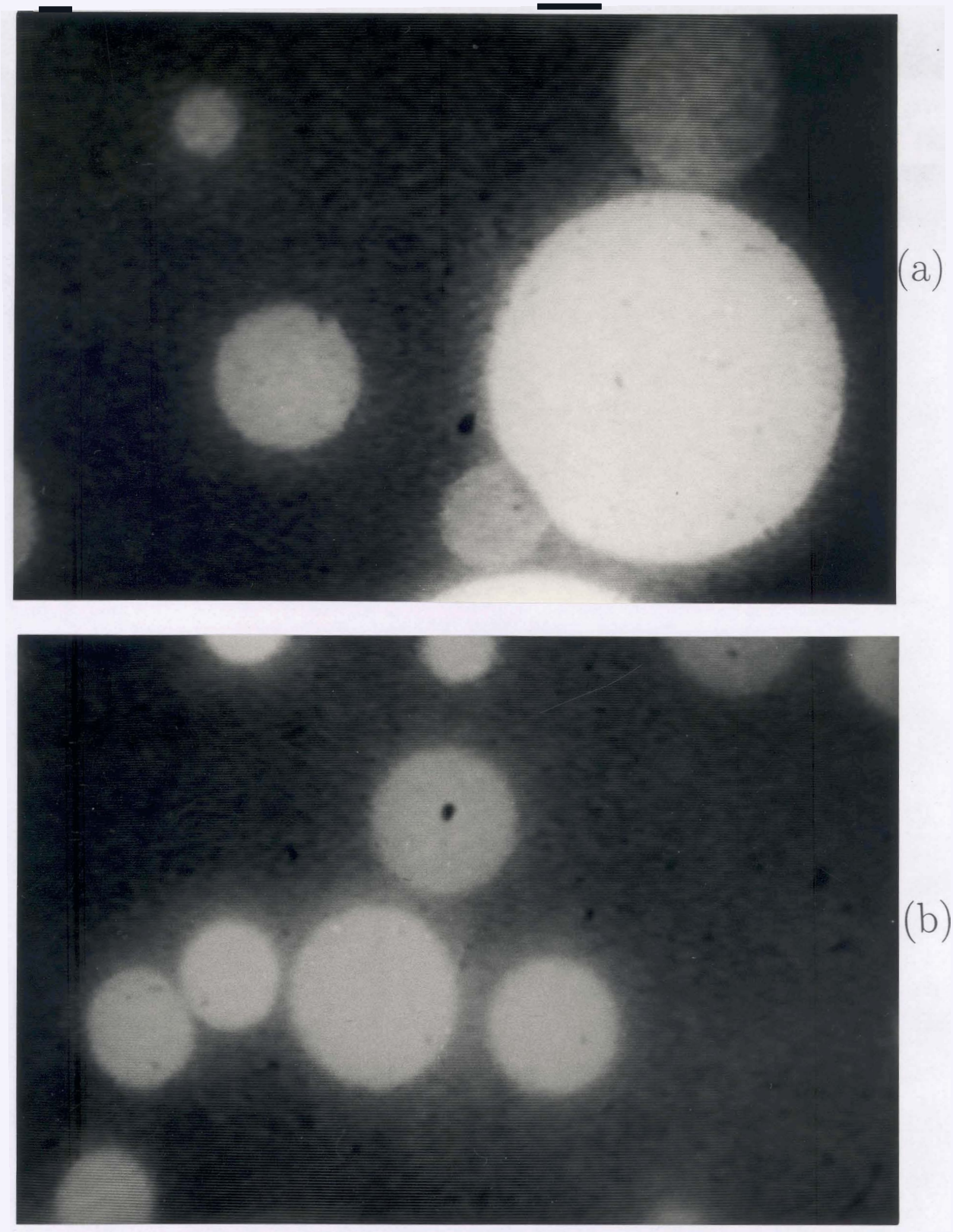

Figure 2.10 Two fluorescence images of co-existing D_2 domains at 25°C. (a) The different D_2 domains are of different intensities, indicating different thicknesses. (b) Here the D_2 domains are of similar size but have different thicknesses. In both the images, the dark background is a D_1 domain. Both the images were taken at $10 Å^2 A_m$. Scale of the images: 1200μm x 800μm.

height difference of 1μm or more between different objects in the field of view. All the D_2 domains were simultaneously in focus with the LE phase and the D_1 domains. So we conclude that they were less than 1μm in thickness. Similar effects were seen upto a temperature of 28°C.

In the temperature range between 28°C and 36°C, the D_1 domains were formed around 45Å^2 on compressing from the pure LE phase. On compressing further, small bright domains (D_3) appeared at 20Å^2 A_m instead of the D_2 domains. The D_3 domains are shown in Fig 2.11. They were brighter than the D_2 domains and much smaller in size. There was a co-existence of the LE phase with the D_1 and D_3 domains. The D_3 domains also appeared near the centre of the D_1 domains. The D_3 domains could not be seen in focus simultaneously with the LE phase or the D_1 domains. This indicated that they were very thick. We measured the thickness of the D_3 domains by focusing the microscope alternately on the D_3 domains and on the LE phase and D_1 domains. In this way, we estimated that the thicknesses of the D_3 domains ranged between 1 and 40 pm.

For temperatures above 36°C, the D_3 domains appeared directly in the LE phase at 45Å^2. Here, the D_1 domains were absent. The D_3 domains co-existed with the LE phase. The D_3 domains were somewhat smaller and thicker than those seen in the temperature range 28°C to 36°C.

On expanding the monolayers, the D_1, D_2 or D_3 domains smoothly changed over to the monolayer in the LE phase, though there was a little hysteresis in the actual π - A, isotherms.

To investigate the surface topography of the D_2 and D_3 domains, we employed reflection microscopy. The LE phase and the D_1 domains were not visible under reflection. The comparatively thicker D_2 domains, which were seen for temperatures below 28°C, exhibited different but uniform colours. As shown in Fig 2.12, they looked like discs of different colours, the colour of each disc being uniform.

On heating beyond 28°C, the domains exhibited concentric interference rings corresponding to their transformation to D_3 domains (Fig 2.13). The presence of the rings in the domains indicated a lens like shape. As the temperature was

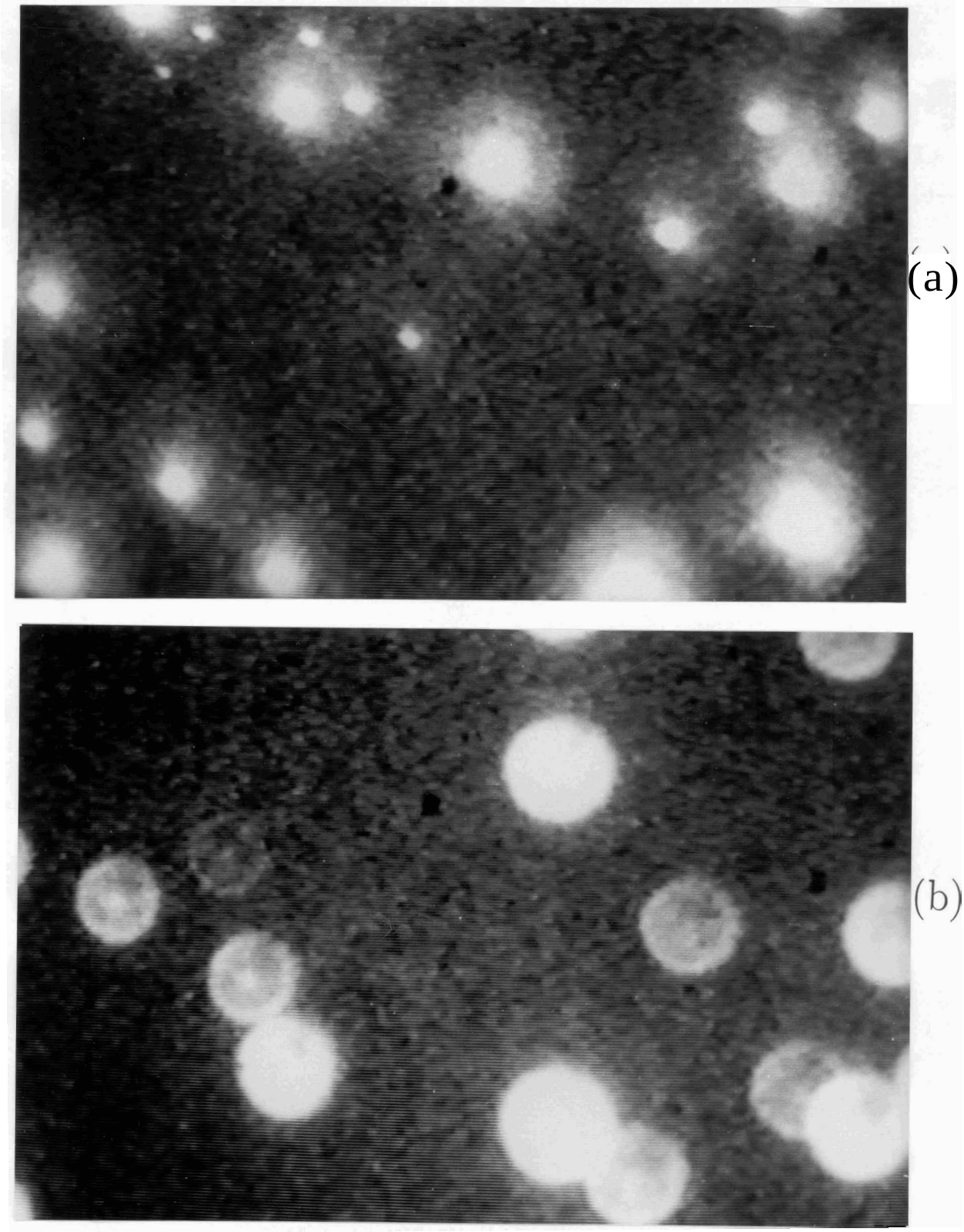

Figure 2.11 Fluorescence images of 8CB monolayer at 32°C, 15 $\text{Å}^2 A_m$. (a) The bright domains are the D_3 domains. As can be seen, the smaller domains and the LE phase are in focus, while the larger ones are out of focus. (b) A similar image. Here, the larger domains are in focus while the smaller ones are out of focus. Scale of the images: 1200μm x 800μm.

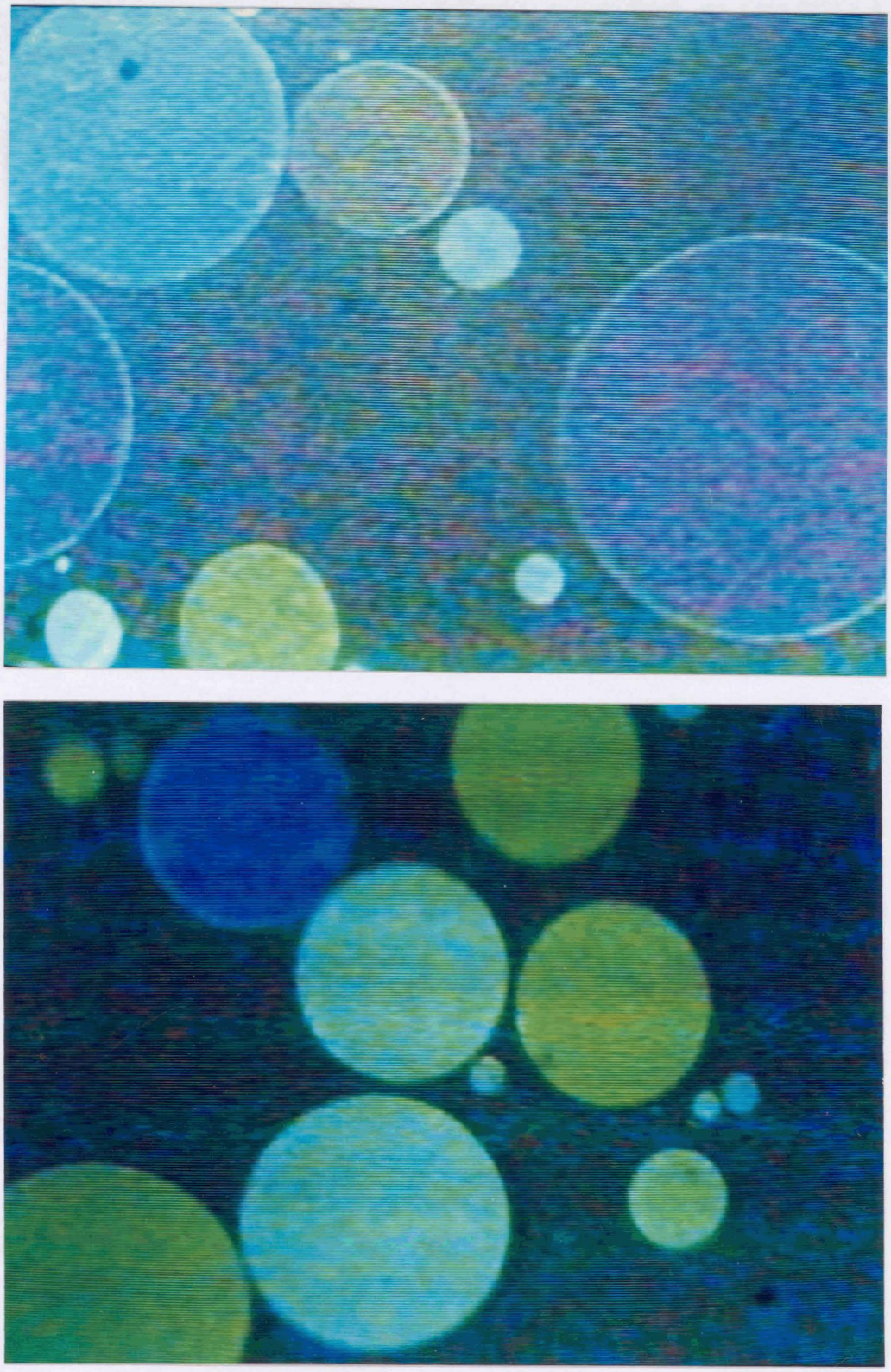

Figure 2.12 Two reflection images of D_2 domains at 25°C, 10Å$^2 A_m$. (a) Each domain is of a uniform colour, indicating that it is optically flat. The different colours of the domains show that they are of different thicknesses. (b) A similar image. Here the D_2 domains are of similar size but different thicknesses. Scale of the images: 1080μm x 800μm.

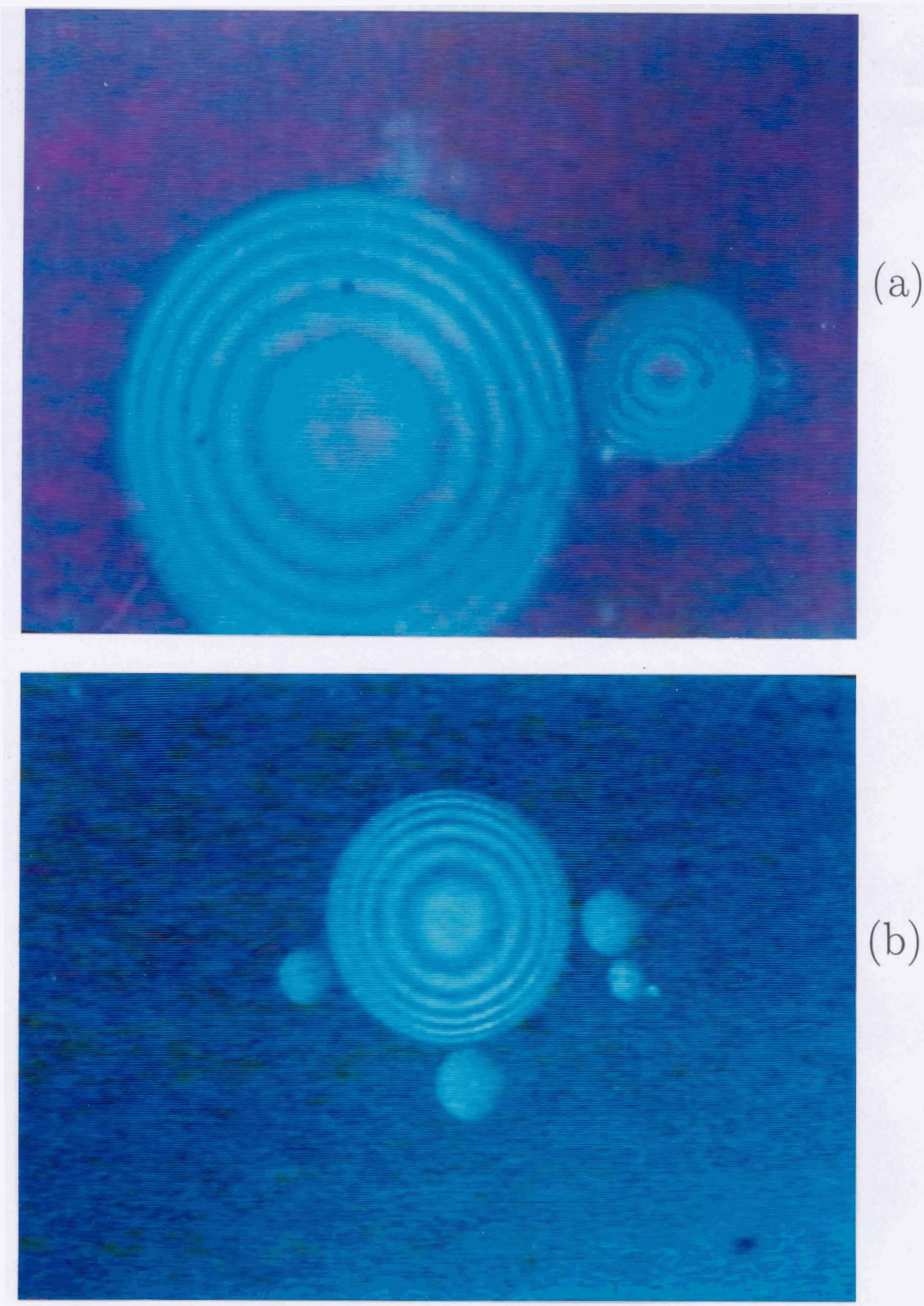

Figure 2.13 Two reflection images of D_3 domains at 30°C, 10 $Å^2 A_m$. (a) The concentric rings are due to interference and indicate a lens like shape. (b) A similar image of a smaller domain. Scale of the image: $1080\mu m \times 800\mu m$.

increased, the domains decreased in size while the number of rings increased. This indicated a growth of the domains in the third dimension. These features were seen for temperatures as high as 45°C.

On cooling, the domains grew in size while the rings decreased in number on approaching 28°C. This indicated a transition from D_3 to D_2 domains as shown in Fig 2.14. Here domains of different colours changed in quick succession as the molecules re-oriented themselves. During this time, some domains showed patches of different colours, probably due to the re-orientation of the molecules. However, these effects were seen only for a short time. Soon the domains showed uniform colours, indicating that the re-orientation was a fast process.

The fluorescence and reflection results were identical, whether the monolayer was first heated and then compressed or first compressed to the necessary A, and then heated.

We studied the monolayer in transmission using a polarising microscope to identify the phases of the D_2 and the D_3 domains. Here again, the LE and D_1 domains were not visible. The D_2 or D_3 domains could be seen only on compressing the monolayer to less than 20Å^2. For temperatures below 28°C, the D_2 domains were large and transparent. These domains were darker than the background and of different shades. The different shades indicated the different thicknesses of the domains. These domains transformed into D_3 domains on heating to 28°C and showed schlieren textures [12], which are typical of a nematic phase (Fig 2.15). In addition, the domains shrank in size. The schlieren textures appeared as small entities at many points in the D_2 domains and grew in size till they joined each other. Here the domains showed a large number of ± 1 defects. The total defect strength of any domain in this stage was +1. On further heating, the defects started collapsing in pairs till there was only one $+1$ or two $+\frac{1}{2}$ defects left. We observed some boojum like textures [13, 14], shown in Fig 2.16. Some of the boojums changed to a normal schlieren texture. Above 36°C, the textures disappeared and the domains became transparent. These domains cast shadows indicating a convex lens like shape.

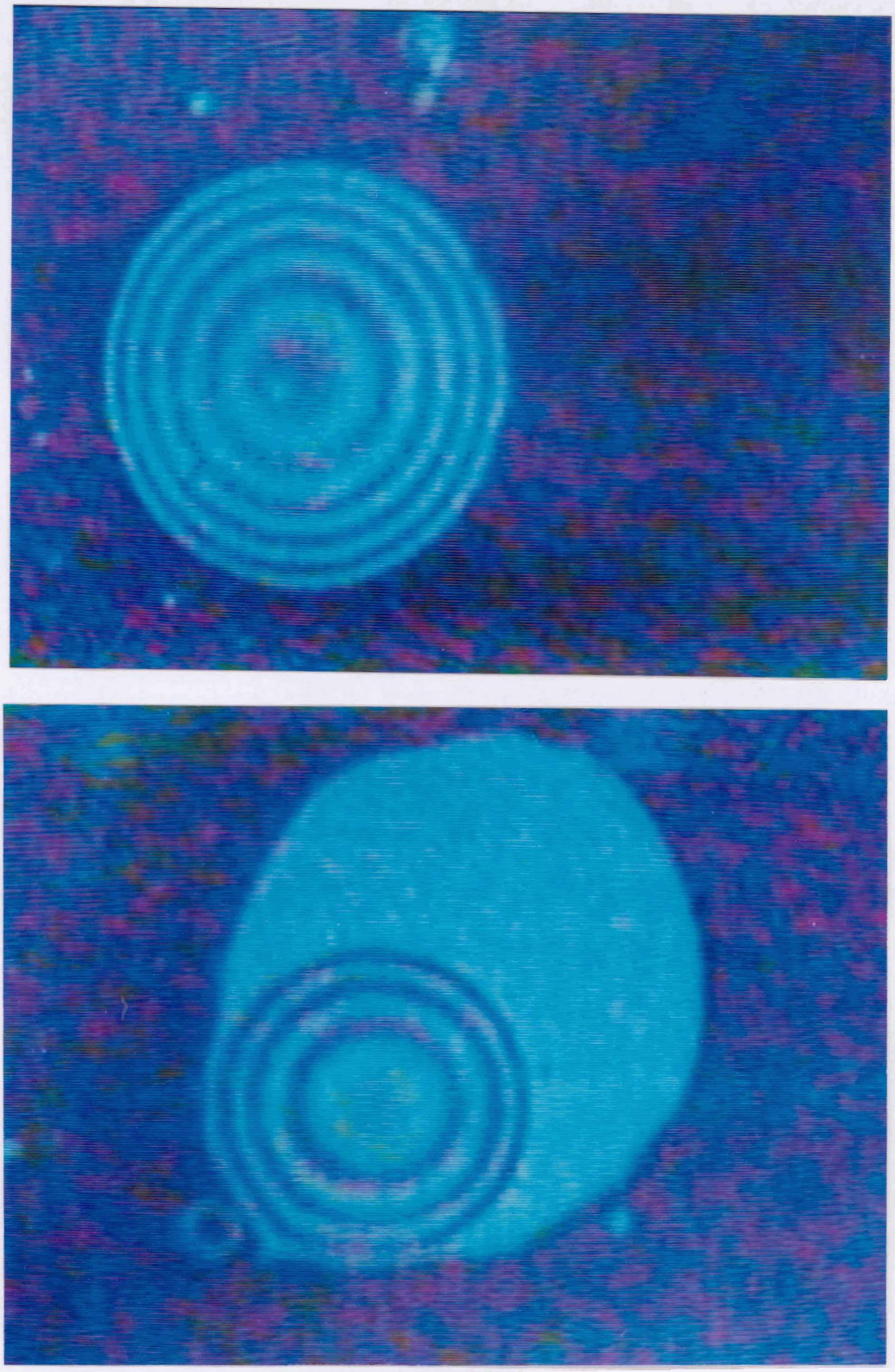

Figure 2.14 (a) A D_3 domain at 30°C under reflection. (b) The same domain at 25°C, a D_2 domain can be seen growing out of it. Scale of the images: 1080μm x 800μm.

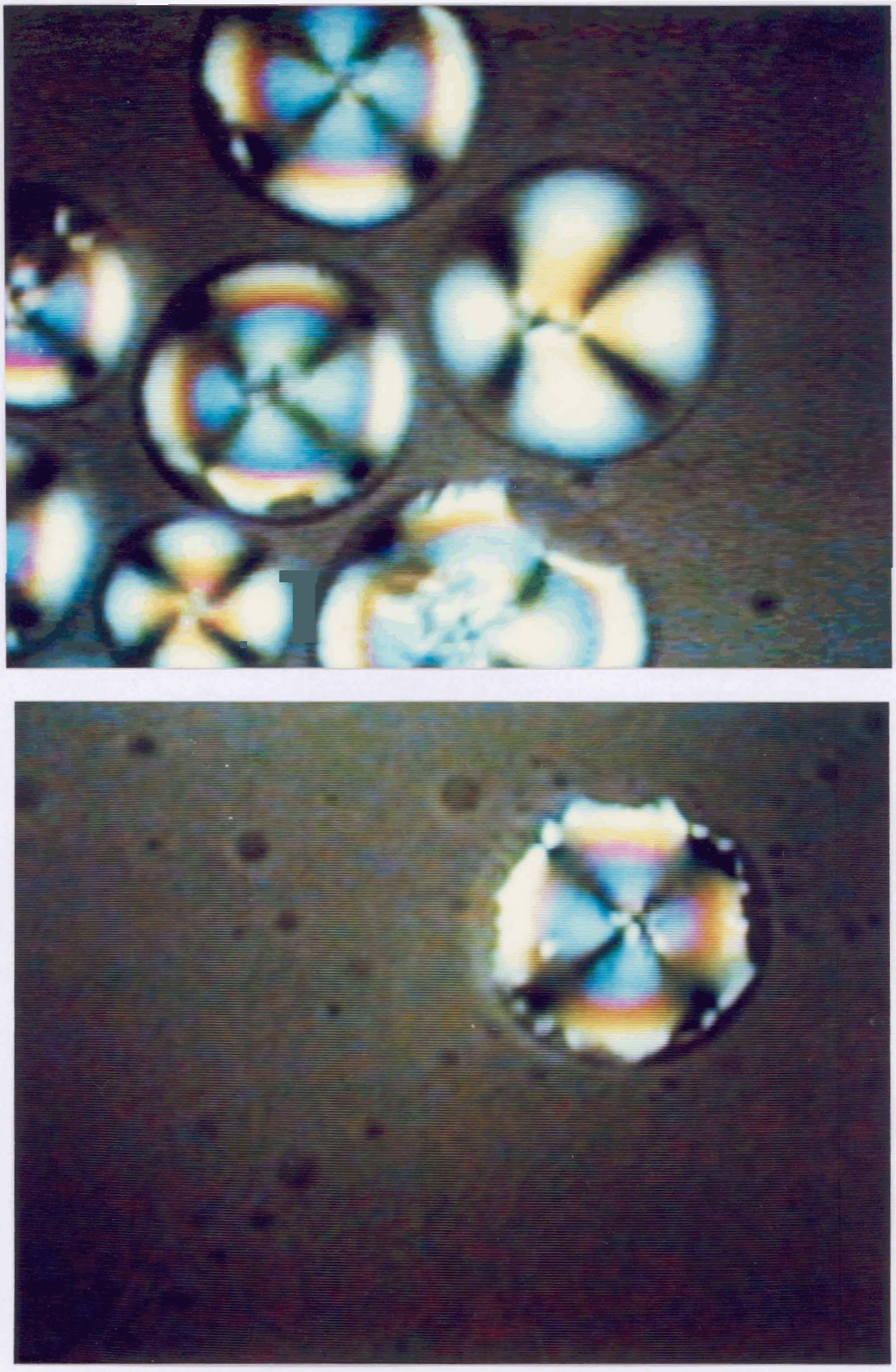

Figure 2.15 Schlieren textures exhibited by D_3 domains at 30°C, seen under a polarising microscope. (a) The domain at the bottom left exhibits a $+1$ defect while that at the right has two $+\frac{1}{2}$ defects. (b) A single domain with a $+1$ defect. Scale of the images: 400μm x 300μm.

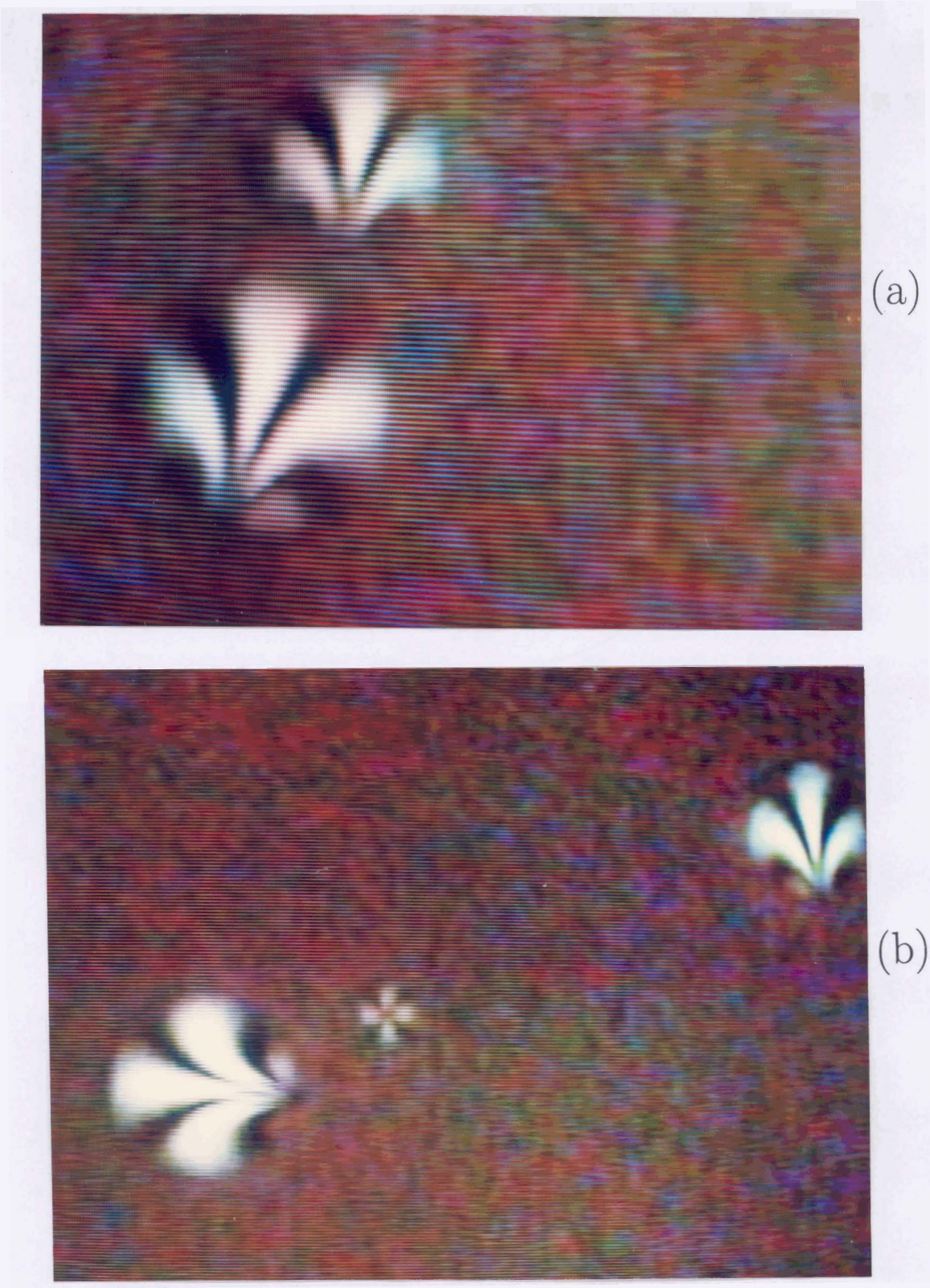

Figure 2.16 Image of D_3 domains at 30°C under a polarising microscope. (a) Two domains exhibiting a boojum texture. (b) Two domains exhibiting boojum texture and one with ordinary schlieren texture. Scale of the images: 400μm x 300μm.

On cooling from this point, the schlieren textures re-appeared at 36°C. The appearance of schlieren textures here was much faster and smoother than what was seen during heating. Again the domains exhibited defects of strength ± 1 and $\pm\frac{1}{2}$ along with boojums. On further cooling, the small D_3 domains changed to larger D_2 domains. The textures disappeared in most of the area of the domains except for a few defects near the periphery of the domains. These defects persisted even after the monolayer was left at room temperature for hours.

In order to distinguish the D_2 domains from the transparent D_3 domains seen for temperatures above 36°C, we studied them by conoscopic technique. The domains were studied under convergent light between crossed polarisers. The D_2 domains exhibited colours of non-uniform intensity. On the other hand, the D_3 domains appeared colourless.

2.4 Discussions

The $\pi - A$, isotherms are identical, irrespective of the time that elapses between the spreading of the monolayer and the starting of the experiment. This indicates that the 8CB molecules do not dissolve in water.

The gas – LE co-existence region corresponds to a horizontal curve in the isotherm, as shown in Fig 2.7. This indicates that the transition is first order. Under the fluorescence microscope, we see the co-existence of the dark gas phase and the bright LE phase. The surface potential AV of the monolayer in this region [7] exhibits fluctuations. This indicates a two phase co-existence. The surface potential changes depending on which phase comes under the electrode.

On compressing, there is onset of the LE phase, where the whole monolayer becomes uniformly bright. This corresponds to the region of steeply increasing π in the isotherm. In this region AV increases linearly [7] with compression so that

$$\text{AVA}, \quad = 25.8\text{V } \text{A}^2 \tag{2.6}$$

This corresponds to an effective dipole moment per molecule

$$P_{\perp} = 0.68 \text{ Debye} \tag{2.7}$$

Since the value of $P_{\perp}$ is constant, it can be inferred that the molecular orientation does not change. The change in π here is due to the increase in the density of molecules. A constant second harmonic signal [4] has also been reported in this region.

The value of π corresponding to the LE – D_1 transition is relatively small (4.5 dyne/cm). This suggests that the surface activity of the material comes from a delicate balance of molecular interactions which can be easily perturbed [5]. This delicate nature of the surface activity is further confirmed by the fact that only the cyanobiphenyls with alkyl chains between 5 and 10 carbons form stable monolayers.

The monolayers of a cyanoterphenyl have been studied by Daniel *et.al.* [15] using surface manometry. This compound is similar to 8CB in structure. It has three phenyl rings instead of two and a hydrocarbon chain with five carbon atoms. The $\pi - A$, isotherms are qualitatively similar to those of 8CB, though the surface pressures are higher. A change of slope similar to the one corresponding to the LE to D_1 transition is reported. These authors conjecture that this is due to a reversible collapse of the monolayer at $23 Å^2$ A, which corresponds to the formation of thicker structures. On compressing to $10 Å^2$ A, they obtain another collapse corresponding to the formation of very thick domains which were visible to naked eye. The behaviour of this compound appears to be similar to 8CB.

Surface manometric studies appear to indicate that the LE to D_1 transition is a first order transition. But, as can be seen in Fig 2.7, the isotherm in the co-existence region is not horizontal. Also, it depends on the compression rate, being close to horizontal for fast compressions, as seen by Xue *et.al.* [4]. According to the Crisp's phase rule, described in Chapter 1, if there is a two phase co-existence, as required for a first order phase transition, there are no degrees of freedom for the system. Hence π should remain constant till the transition is complete. So the

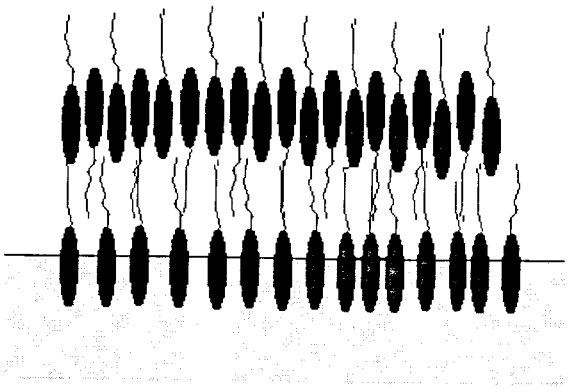

Figure 2.17 Schematic diagram of the molecular arrangement in a three layer domain.

isotherm should show a flat region independent of the compression rate. However, as seen in Fig 2.7, there is a steady increase in π on compression. Also, the D_2 or D_3 domains appear before the D_1 domains fill up the entire interface, as seen in Fig 2.9 and 2.11 (b). This is contrary to the expectations for a first order phase transition. In fact, at temperatures above 36°C, the D_1 domains do not appear at all. All these indicate that D_1 is an unstable structure and hence can not be called a separate phase.

Another point to be noted here is the co-existence of the LE phase with the D_1 and D_2 domains or the D_1 and D_3 domains. Such a three phase co-existence is not permissible for a single component monolayer according to the phase rule. This also tends to indicate that the D_1, D_2 and D_3 domains are unstable structures.

The value of AV remains constant [7] over the LE – D_1 co-existence region, indicating that the dipole moment per unit area is not changing. This indicates that the bilayer forming on top of the monolayer is not contributing to the dipole moment. This suggests that it has an interdigitated structure so that the component of the dipole moment normal to the interface is getting cancelled. This is a direct proof that the D_1 domains are 3 layer and not 2 layer as in that case one would expect for a change in ΔV.

The mechanism of transformation of the monolayer into a three layer structure

has been described by Mul and Mann [6]. Unlike in ordinary monolayers, here the transformation takes place in a very orderly manner and we obtain circular multilayer domains. The monolayer buckles into a bilayer, in which the headgroups get interlocked to form an interdigitated structure. This interdigitated bilayer ultimately settles over the monolayer [16]. This gives rise to a three layer structure as shown in Fig 2.17. Such interdigitation occurs due to the strong dipolar interaction between the cyano groups. This has been reported in cyanobiphenyls, including 8CB, in bulk. The length scale of the nucleation is less than 1pm. These bilayer domains assume a circular shape and grow uniformly till they are closely packed.

The change from the three layer to higher multilayers is not so orderly. This can be inferred from the presence of multilayers of many different thicknesses at the same time. It is possible that this transformation also followed a similar mechanism. In a recent paper, Mul and Mann [17] report their studies on the thickness of the multilayer films of 8CB. Their studies indicate the presence of 5 and 7 layer domains in the film.

The D_2 domains, seen for $A, < 20\text{Å}^2$ below 20°C are optically flat structures, as can be made out from the uniform colours shown in reflection. These domains are less than $1\mu\text{m}$ thick, as they focus in the same plane with the LE and the D_1 domains. The fact that they are visible under reflection suggests that their thickness is at least 0.2 pm as implied by Equation 2.5. The D_2 domains are textureless in parallel light transmission and they show non-uniform colours when illuminated in transmission by convergent light. So we can conclude that they are in the smectic A phase with homeotropic geometry, *i.e.* with the molecules oriented normal to the water surface. This is why they do not show any textures under parallel light transmission, as the light passes along the optic axis. The domains are birefringent to convergent light as this light does not pass along the optic axis, as shown in Fig 2.6 (b). This indicates that the 8CB molecules are anchored to the water surface and have a homeotropic alignment. This anchoring may also account for the fact that the domains never grow beyond 1pm in

thickness.

The D_3 domains seen between 28°C and 36°C show a schlieren texture, suggesting that they are in the nematic phase. These domains are much thicker (1 to 40 μm) than the D_2 domains. This indicates that the anchoring of the molecules to the subphase weakens at higher temperatures. The domains are convex lens shaped with a total defect strength of $+1$, seen either as two $+\frac{1}{2}$ defects or a single $+1$ defect. These defects occur as the molecules inside the domain are free to move about and the molecules near the edge of the domain align themselves normal to the surface. While in most cases the defects occur near the centre of the domain, some domains have the defect at an edge, giving a boojum structure. Some of the domains with the boojum structure change into the standard schlieren texture with the defect at the centre. This indicates a weak anchoring of the domains to the subphase.

The D_3 domains seen for temperatures above 36°C are in the isotropic phase. This can be seen from the fact that they are textureless under both parallel and convergent light transmission. Their shadows indicate that they are of a convex lens shape.

On cooling the domains, the isotropic to nematic transition is smooth and easy to detect. On the other hand, in the transition from nematic to smectic A, we observe small regions with some textures in the D_2 domains formed on cooling. So the texture change is not complete. This may be due to some kind of reluctance of the molecules to go into the homeotropic geometry. The transition temperatures for both the heating and cooling cycles are the same.

$$Smectic A \xrightarrow{28^{\circ}C} Nematic \xrightarrow{36^{\circ}C} Isotropic.$$

The different transition temperatures are lower than the corresponding ones for bulk 8CB, though the phase sequence is the same. These transition temperatures are reproducible and do not depend on the thickness of the subphase. This reduction in the transition temperatures may be due to the presence of water in

the bilayers making up the domains. According to Xue *et.al.*, [4] water molecules can penetrate some distance up into the alkyl chains of the molecules forming the monolayer. Since the alkyl chain of 8CB is short, there is a possibility that a large amount of water may be present near the monolayer air interface. They have confirmed this phenomenon by observing that the monolayer and three layer films did not wet oil (hexane, hexadecane etc.), which is a sign of presence of water. The presence of water has also been suggested by Mul and Mann [6].

Enderle *et.al.* [18] have conducted surface manometry and second harmonic generation (SHG) studies on 8CB monolayer at room temperature. They report no SHG signal from the monolayer for A, $> 50Å^2$. This is followed by a region with strong SHG signal ($50Å^2$ to $40Å^2$ A,). On compressing beyond A, = 40 $Å^2$, the SHG signal starts decreasing. From our results, we suggest that for A, $> 50Å^2$, the molecules are in the gas phase and are randomly oriented. As a result, the structure is effectively centrosymmetric, hence no SHG signal is obtained. In the range between 50 and $40Å^2$ A,, the monolayer is predominantly in the LE phase, which is non - centrosymmetric. Hence one gets a strong SHG signal. For A < 40 $Å^2$, the 8CB molecules start forming D_1 domains with smectic A order, which possesses a centre of symmetry. This results in a reduction of the SHG signal.

Schmitz and Gruler [7] report an additional phase transition at $17Å^2$, where the AV – A, curve shows a change of slope and starts decreasing. This transition is not detected by surface manometry. It appears to be a second order transition as there is only a decrease in the slope of the AV – A, curve. The value of A, corresponds to the region of co-existence of LE, D_1 and D_2 domains. The authors explain this change in the AV curve to be due to the D_1 domains coming into contact with each other, which occurs around this value of A,. As a result the electrodes see less of the bare monolayer and hence there is drop in AV.

Mul and Mann [19] have studied multilayers of 9CB and 10CB, the two next homologues of 8CB using Brewster angle microscopy. The $\pi - A$, isotherms of these compounds are almost identical to those of 8CB. Also, they observe the

formation of 3 -layer and multilayer domains, which are unstable structures.

Schroter *et.al.* [20] have studied a set of rod – like liquid crystal molecules which have a hydrophilic group attached laterally. Their results show a similar transition from the monolayer to a three layer structure, which they suspect to be a first order transition. However, here the arrangement of molecules in the three layer structure is different. The molecules are oriented parallel to the interface, with the middle and top layers facing each other. It is interesting to note that a molecule with a terminal hydrophilic attachment like 8CB and a molecule with a lateral attachment behave in a similar manner.

In a recent study, Sakamoto *et.al.* [21] have studied the 8CB film in the LE – D_1 co-existence region using Ripplon light scattering and convergent ellipsometry around the Brewster angle. Using these techniques, they determine the elastic constant ε of the D_1 domains to be 2 x 10^{-1}N/m and of the LE phase as 4 x 10^{-2}N/m. This is contrary to the simplest model of a three layer which predicts

$$\frac{\varepsilon_{D1}}{\varepsilon_{LE}} = 3 \tag{2.8}$$

Instead they obtain

$$\frac{\varepsilon_{D1}}{\varepsilon_{LE}} > 5 \tag{2.9}$$

This indicates that the D_1 domains result in a hard film with very high elasticity. They also study the relative thicknesses d of the LE and the D_1 structures and find that

$$\frac{d_{D1}}{d_{LE}} = 2 \tag{2.10}$$

against the simplest model prediction

$$\frac{d_{D1}}{d_{LE}} = 3 \tag{2.11}$$

This indicates that the two upper layers of the D_1 domains are highly interdigitated. Also, the LE to D_1 transition begins at A, $\sim 48\text{Å}^2$ and continues to

20 Å^2, and is not complete even there. The large ratio between the A, values at these two points appears to indicate that the upper bilayer has a very high surface density compared to the monolayer.

We find that the transition from LE to the 3D domains is reversible, though there is some hysteresis in the $\pi - A$, isotherms. Friedenberg *et.al.* *[5]* observe a few thick droplets even after the monolayer has been expanded the the region corresponding to the steep decrease in π in their Brewster angle microscopy studies. They attribute the hysteresis partly to this residual multilayer content. The hysteresis could also be due to some 8CB molecules getting attached to the edges of the trough and the barrier, and hence not contributing to the monolayer.

Interestingly, the 3D domains transform to the LE phase smoothly on expansion, irrespective of the temperature. So, it appears that the transition between the monolayer and the 3D islands results from a competition between the energy of adsorption at the air water interface and the cohesive intermolecular forces of the bulk phases. The mechanical compression of the monolayer provides a mechanism to continuously vary the energy of adsorption at the air – water interface. At high surface molecular density, the energy of adsorption at the interface becomes weaker as the molecules change their orientation. This seems to favour the formation of the 3D phases.

2.5 Conclusions

Our studies indicate that the 8CB monolayer evolves continuously into a liquid crystalline phase on compression. This transition of a 2D monolayer into a 3D liquid crystalline phase on compressing and the reverse transition on expanding indicates that the molecular organisation can be continuously tuned by the surface molecular density.

We may interpret that the molecular interactions stabilising a monolayer dominates for low surface density. This results in an adhesion of the molecules to the subphase. On increasing the surface density, the interactions that lead to the

formation of liquid crystals take over and a 3D cohesion of the molecules sets in.

These 3D domains exhibit liquid crystalline order. The phases that occur in these domains are the same as those in bulk 8CB, but the transition temperatures are lower. This decrease in the transition temperatures appears to be due to the presence of water molecules in the domains.

Bibliography

[1] H. D. Dorfler, W. Kerscher and H. Sackmann *Z.* Phys. Chem, 251, 314 (1972).

[2] K. A. Suresh, A. Blumstein and F. Rondelez, **J.** Physique 46, 453 (1985).

[3] A. Ulman, An Introduction to Ultrathin Organic Films; Academic Press; San diego, CA (1991).

[4] J. Xue, C. S. Jung and M. W. Kim, Phys. Rev. Lett., 69, 474 (1992).

[5] M. C. Friedenberg, G. G. Fuller, C. W. Frank and C. R. Robertson, Langmuir 10, 1251 (1994)

[6] M. N. G. de Mul and J. A. Mann Jr. Langmuir 10, 2311 (1994).

[7] P. Schmitz and H. Gruler, *Europhys.* Lett., 29, 451 (1995)

[8] A. Pockels, Nature, 43, 437 (1893).

[9] I. Langmuir, **J.** Am. Chem. *Soc.*, 39, 1848 (1917).

[10] G. L. Gaines Jr., Insoluble Monolayers at Liquid Gas Interface, (Interscience, New York) 1966.

[11] C. M. Knobler, Adv. Chem. Phys., 77, 397 (1990).

[12] D. Demus and L. Richter, Textures in Liquid Crystals; Verlag Chemie; Weinheim and New York, 1978.

[13] S. Riviere and J. Munier, Phys. Rev. Lett., 74, 2495, (1995).

[14] P. Galatola and J. B. Fournier, Phys. Rev. Lett., 75, 3297 (1995).

[15] M. F. Daniel, O. C. Lettington and S. M. Small, Thin Solid Films, 99, 61 (1983).

[16] H. E. Ries Jr., Nature, 281, 287 (1979).

[17] M. N. G. de Mul and J. A. Mann Jr., Langmuir, 14, 2455 (1998).

[18] Th. Enderle, A. J. Meixner and I. Zschokke-Granacher *J.* Chem. Phys., 101, 4365 (1994).

[19] M. N. G. de Mul and J. A. Mann Jr., Langmuir, **11,** 3292 (1995).

[20] J. A. Schroter, R Plehnert, C Tschierske, S. Katholy, D. Janietz, F. Penacorada and L. Brehmer, Langmuir, 13, 796 (1997).

[21] N. Sakamoto, K Sakai and K. Takagi, Phys. Rev. E, 56, 1838 (1997).